AD_____

Award Number: W81XWH-11-1-0510

TITLE: Early Detection of Ovarian Cancer by Molecular Targeted Ultrasound Imaging Together with Serum Markers of Tumor-Associated Nuclear Change and Angiogenesis

PRINCIPAL INVESTIGATOR: Animesh Barua, Ph.D.

CONTRACTING ORGANIZATION: Rush University Medical Center
Chicago, IL 60612

REPORT DATE: October 2012

TYPE OF REPORT: Annual

PREPARED FOR: U.S. Army Medical Research and Materiel Command
Fort Detrick, Maryland 21702-5012

REPORT DOCUMENTATION PAGE

Form Approved
OMB No. 0704-0188

1. REPORT DATE	2. REPORT TYPE	3. DATES COVERED
30 October 2012	Annual	30 September 2011- 29 September 2012

4. TITLE AND SUBTITLE
Early Detection of Ovarian Cancer by Molecular Targeted Ultrasound Imaging Together with Serum Markers of Tumor-Associated Nuclear Change and Angiogenesis

5a. CONTRACT NUMBER

5b. GRANT NUMBER
W81XWH-11-1-0510

5c. PROGRAM ELEMENT NUMBER

6. AUTHOR(S)
Animesh Barua, Ph.D.

E-Mail: Animesh_Barua@rush.edu

5d. PROJECT NUMBER

5e. TASK NUMBER

5f. WORK UNIT NUMBER

7. PERFORMING ORGANIZATION NAME(S) AND ADDRESS(ES)

Rush University Medical Center,
Chicago, IL 60612

8. PERFORMING ORGANIZATION REPORT NUMBER

9. SPONSORING / MONITORING AGENCY NAME(S) AND ADDRESS(ES)
U.S. Army Medical Research and Materiel Command
Fort Detrick, Maryland 21702-5012

10. SPONSOR/MONITOR'S ACRONYM(S)

11. SPONSOR/MONITOR'S REPORT NUMBER(S)

12. DISTRIBUTION / AVAILABILITY STATEMENT
Approved for Public Release; Distribution Unlimited

13. SUPPLEMENTARY NOTES

14. ABSTRACT
One of the most significant barriers to establishing an early ovarian cancer (OVCA) detection test is the difficulty of identifying patients with early stage OVCA. In earlier approaches to develop an early detection test for OVCA, using serum levels of CA-125, traditional transvaginal ultrasound and their combination did not improve the detection of OVCA remarkably. The limitation of CA-125 is that it is non-specific in detecting OVCA at the early stage and no imaging target(s) in the ovary corresponding to the elevated serum CA-125 levels has been defined. Our overall goal is to establish an early detection test for OVCA using vascular endothelial growth factor receptor -2 (VEGFR-2) targeted ultrasound molecular imaging in association with serum anti-nuclear matrix protein (anti-NMP) antibodies (a marker of tumor associated nuclear change) and serum IL-16 levels (a marker of ovarian tumor-associated neoangiogenesis, TAN). This goal is being achieved by two specific aims. The results of Aim 1 suggest that VEGFR-2 targeted ultrasound imaging enhances the detection of ovarian tumors in the laying hen model of spontaneous OVCA. Changes in OVCA related VEGFR-2 targeted imaging indices are associated with the prevalence of serum anti-NMP antibodies and the elevation of serum IL-16 levels.

15. SUBJECT TERMS- Ovarian cancer, Early detection, Ultrasound molecular imaging, VEGFR-2, animal model

16. SECURITY CLASSIFICATION OF:			17. LIMITATION OF ABSTRACT	18. NUMBER OF PAGES	19a. NAME OF RESPONSIBLE PERSON
a. REPORT	b. ABSTRACT	c. THIS PAGE			USAMRMC
U	U	U	UU	13	19b. TELEPHONE NUMBER *(include area code)*

Table of Contents

Page

INTRODUCTION:

Ovarian cancer (OVCA) is the leading cause of death of women due to gynecological cancers [1]. While the survival rates of OVCA patients are remarkably high if the disease is detected at early stage (>80%), most cases of OVCA are diagnosed at late stages when the likelihood of successful therapy is very low [2]. Non-specificity of symptoms at the early stage and the lack of an effective and specific early detection test make the diagnosis of OVCA at the early stage very difficult. Serum levels of CA-125 and traditional transvaginal ultrasound (TVUS) scanning are the currently available tests for the detection of OVCA. A combination of CA-125 and TVUS scanning failed to effectively detect OVCA at the early stage as circulating levels of CA-125 are non-specific to OVCA and traditional TVUS scanning cannot detect early OVCA related changes in the ovary [3]. Thus a fresh approach is needed. Malignant nuclear transformation and tumor associated neoangiogenesis (TAN) are two of the earliest events in tumor initiation and development. During malignant transformation, the nuclei of cells undergo profound morphological changes in size and shape together with rearrangements in nuclear matrix proteins (NMPs). As a result, NMPs are shed into the circulation, in response to which the immune system produces anti-NMP antibodies. These NMPs and their corresponding anti-NMP antibodies are tissue specific [4]. Malignant nuclear transformation is followed by ovarian TAN. Development of angiogenic microvessels is the characteristic feature of ovarian TAN. These microvessels express vascular endothelial growth factor receptor-2 (VEGFR-2) which is an accepted marker of angiogenesis. Thus, serum anti-NMP antibodies and VEGFR-2 expressed by TAN vessels in the ovary represent potential markers for early ovarian tumor related changes, to be detected by serum analysis and by *in vivo* imaging, respectively, if an *in vivo* imaging probe can be developed. Although traditional Doppler ultrasound (DUS) scanning detects ovarian vascular structures, its limited resolution cannot detect early stage OVCA related ovarian TAN vessels. Our long term goal is to improve the detectability of ovarian TAN vessels at early stage OVCA by molecular targeted (VEGFR-2) contrast enhanced ultrasound imaging. Due to the difficulty in identifying patients with early stage OVCA, in this project we are using laying hen model of spontaneous OVCA to achieve our goals [5, 6]

BODY: the research accomplishments associated with each task outlined in the approved Statement of Work.

The overall hypothesis of this project is that *early stage OVCA lesions can be detected in laying hens using VEGFR-2 targeted contrast enhanced ultrasound imaging in association with anti-NMP antibodies and serum levels of IL-16.* This hypothesis is being tested with the following two specific aims: 1) Molecular targeted-ultrasound imaging will identify hens with early stage OVCA and 2) VEGFR-2 targeted-ultrasound acoustic indices (AI) and TAN indices (TI) established in Aim 1 will detect ovarian TAN in hens with anti-NMP antibodies.

Task 1. Molecular targeted-ultrasound imaging of hen ovarian tumors and tumor associated neoangiogenesis (TAN)

1a. Scanning of 150 hens to detect ovarian tumor associated abnormalities.

i) Molecular imaging probes containing VEGFR-2 targeted microbubbles were supplied by Targeson, Inc., San Diego, CA.

ii) Detection of ovarian tumors by molecular imaging using molecular probes containing VEGFR-2 targeted microbubbles with gray scale ultrasound scanning;

iii) Detection of ovarian tumor associated microvessels (TAN vessels) by contrast enhanced ultrasound;

iv) Blood was collected from the brachial vein of each hen before ultrasound scan, serum was separated and aliquots were stored at -80^{0}C until further use;

v) Following ultrasound scanning, hens were sacrificed, presence of OVCA and its stages were diagnosed, ovaries with or without tumors and other relevant tissues were harvested, processed for paraffin, frozen, proteomic and molecular biological studies.

1b. Ovarian histopathology and immunohistochemical studies

i) Histopathological diagnosis of OVCA: representative paraffin sections of 5μm thick from ovaries with or without gross tumors were made, stained with hematoxylin & eosin and examined under a light microscope. Presence of ovarian carcinoma on the sections and their histological types were determined.

ii) Paraffin sections were examined for immunohistochemical determination of VEGFR-2 and smooth muscle actin (SMA) expressing angiogenic microvessels using anti-chicken VEGFR2 and anti-SMA antibodies. Similarly, immunopositive CD8 T cell and IL-16 expressing cells/vessels were determined in frozen sections by anti-Chicken CD8 and anti-chicken IL-16 antibodies.

iii) Immunostained sections were examined, the frequencies of immunopositive CD 8+ T and IL-16 cells were determined, correlation between the frequencies of immunopositive cells (markers of ovarian TAN) and tumor stages and tumor sub-types was determined.

1c. Biochemical and molecular biological as well as processing of archived ultrasound imaging data.

i) Serum prevalence of anti-NMP antibodies and circulatory levels of IL-16 in hens with or without ovarian tumors were determined by immunoassay.

ii) Gene expression of IL-16 by normal and tumor bearing hen ovarian tissues was determined by semi-quantitative RT-PCR using chicken IL-16 primers.

iii) Archived pre- and post-targeted ultrasound images were analyzed off-line and contrast parameters or imaging indices detective of early stage ovarian cancer were determined with reference to gross and histopathological observations.

iv) Correlation among the molecular targeted imaging parameters and serum anti-NMP antibody status as well as IL-16 levels detective of OVCA at early stage were examined.

Task 1 milestone: Indices for early stage OVCA comprising molecular targeted ultrasound imaging parameters in association with serum anti-NMP antibodies and IL-16 levels are established.

Task 2: The indices for early detection of OVCA determined from Task 1 are being used in a prospective study. At the end of the study, the specificity and sensitivity of early detection test will be determined.

Detailed Reports on the Accomplishments:

Specific Aim 1: Molecular targeted-ultrasound imaging differentiates hens with early stage OVCA from hens with normal ovaries.

Animals:

3-year old 150 White Leghorn hens with low egg laying rates, (<125eggs/year) and 40 hens with normal egg laying rates (>250eggs/year) were selected from a flock of laying hens. In the first study, an additional 20 hens were selected and divided into two groups (10 hens each) and injected with non-targeted microbubbles or Optison^{TM} and compared with those injected with VEGFR-2 targeted microbubbles. The binding specificity of VEGFR-2 targeted microbubbles was determined and a dose of 10uL/kg body weight was found to be optimal. In the subsequent study, selected hens were injected with 10uL/kg body weight of VEGFR-2 targeted microbubbles via the left brachial vein. All selected hens were reared under identical environmental conditions

and provided with food and water *ad libitum*. Blood from all hens was collected prior to ultrasound imaging and sera were obtained and aliquots were stored at -80 ºC for later use.

Molecular (VEGFR-2) targeted contrast enhanced imaging: *Sonography and Image Analysis*

Pre-targeted imaging: Sonographic imaging was performed before the injection of VEGFR-2 targeted microbubbles with the mechanical set up reported previously [7, 8]. Briefly, all hens were scanned using an instrument equipped with a 5- to 7.5-MHz endovaginal transducer (MicroMaxx; SonoSite, Inc, Bothell, WA). Following immobilization of each hen, the transducer was inserted transvaginally and 2-dimensional (2D) transvaginal gray scale and pulsed Doppler sonographies were performed. Ovarian morphology was examined by gray scale sonography while ovarian vasculature was examined by DUS imaging. DUS imaging indices including the resistive index (RI: [systolic velocity – diastolic velocity]/systolic velocity) and the pulsatility index (PI: [systolic velocity – diastolic velocity]/mean) were automatically calculated from at least two separate images from the same ovary.The lower RI and PI values were used for analysis. All images were processed and digitally archived.

VEGFR-2 targeted imaging:

Targeted imaging was performed following the injection of ovarian VEGFR-2 targeted microbubbles in a similar manner with identical mechanical settings as described above and the same pre-targeted area was imaged according to the instruction of the manufacturer of the targeted agent and earlier report [9]. Within 5-7 min from the arrival, targeted microbubbles were accumulated at the target sites and unbound free microbubbles were washed out. All images were archived digitally in a still format as well as in real-time clips (15 minutes for each hen). The effects of targeted microbubbles were visually evaluated online during the scanning examination and off-line afterward by reviewing the archived still images and video clips. The time of contrast agent arrival (interval in seconds from administration of the contrast agent to its visual observation [in seconds]) in the ovaries with or without tumor was recorded in real time. After review of the complete clip, the region of interest (ROI) was selected. The average image intensity (in pixel values) over a ROI encompassing the tumor was calculated using a computer assisted software (Microsuite^{TM} version Five, Olympus America, Inc., Canter Valley, PA) and compared with the intensity of the pre-targeted imaging of the same ROI. The pixel intensities of ROI predictive of OVCA were determined. In addition, RI and PI values from post-targeted imaging were calculated.

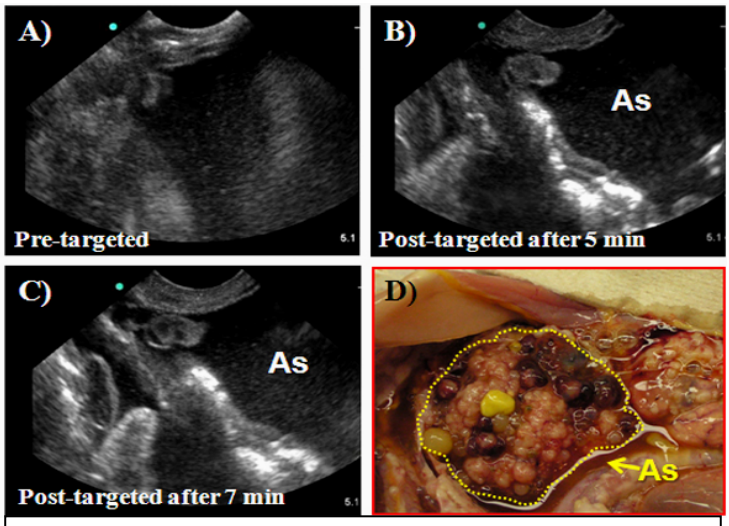

Figure 1. Detection of ovarian tumor by VEGFR-2 targeted ultrasound molecular imaging. A) Pre-contrast gray scale ultrasound image of a hen ovary suspected to have tumor. Intensity of the signals from the tissue is very low. B) Gray scale image of the same ovary 5min after the injection of VEGRF-2 targeted imaging agent. Compared with pre-targeted, signal intensity from the tissue was enhanced remarkably (appears like a white triangular-shaped island of solid mass). C) Gray scale image of the same ovary 7min after the injection of targeted imaging agent showing larger tumor mass with enhanced signal intensity. D) Gross ovarian tumor (dotted line) in the hen scanned in A-C confirming the prediction of targeted ultrasound molecular imaging. As = ascitic fluid.

Result: Representative molecular targeted ultrasonograms of a suspected ovarian tumor in a hen before and after the injection of VEGFR-2 targeted microbubbles are shown in **Figure 1** (Gray scale, showing tumor). One or two large preovulatory follicles together with several small growing follicles were seen during the ultrasound imaging in normal

ovaries in healthy hens (n = 20 selected hens) with low egg laying rates. Compared with pre-targeted scanning, VEGFR-2 targeted imaging enhanced the visualization of solid masses in the ovaries of 26 hens on gray scale and these hens were "suspected to have ovarian malignant tumors" (**Figure 1A-D**). Overall, in contrast to the pre-targeted scan, the pixel intensities of the signals from normal ovaries or ovaries with tumor increased significantly after the injection of VEGFR-2 targeted microbubbles. The mean signal intensity of VEGFR-2 targeted ovarian sonograms for low laying healthy hens was 60352.00 ± 21259.33 (mean ± SD) pixels and it was significantly higher in hens in which tumor masses limited to a part of the ovaries (early stage) 104479.80 ± 28295.62 (mean ± SD) pixels. The signal intensities increased further in hens with large solid ovarian masses accompanied with profuse ascites and predicted to have late stage OVCA, 112989 ± 13373.19 (mean ± SD) pixels. Blood vessels were detected in the ovarian stroma by color Doppler ultrasound imaging. The mean pre-targeted RI values for hens with normal, with small or large ovarian masses were 0.58 ± 0.12, 0.56 ± 0.11and 0.40 ± 0.04, respectively. The RI values were found to be decreased in all hens to 0.47 ± 0.12 (normal), 0.43 ± 0.08 (early stage) and 0.33 ± 0.05 (late stage), respectively, in post-targeted color Doppler ultrasound imaging. Similar patterns were also observed for PI values.

Ovarian histopathology and immunohistochemical studies:

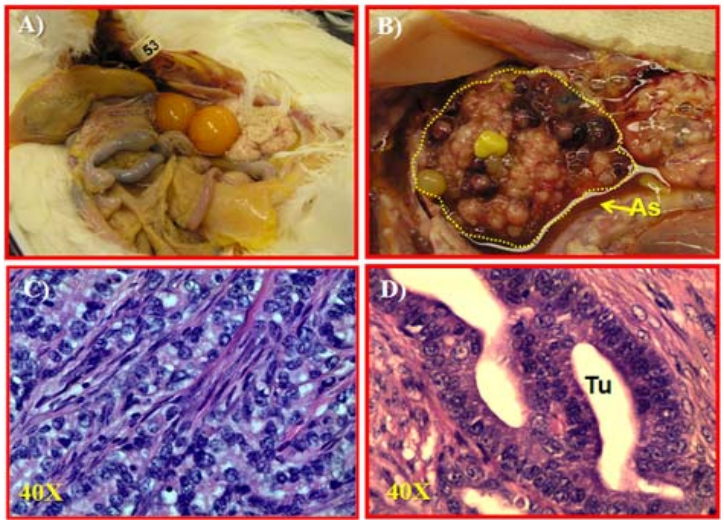

Figure 2. Spontaneous ovarian malignant tumors in hens diagnosed by VEGFR-2 targeted ultrasound molecular imaging. A) A normal ovary in an old laying hen with low egg laying rates. The ovary had two developing pre-ovulatory follicles as opposed to 5-6 follicles seen in a younger laying hen with normal egg laying rates. B) An ovarian tumor at late stage in a laying hen (tumor limited to the ovary). The tumor appears like a cauliflower. C-D) Examples of histological types of malignant ovarian tumors in hens detected in this study. (C) Serous ovarian tumor appears like a sheet of malignant cells with pleomorphic nuclei surrounded by fibromuscular layer. D) An endometrioid ovarian tumor showing back to back tumor glands (Tu) resembling those seen in endometrium with a single layer of epithelial cells and sharp luminal lining. Dotted line shows the tumor. 40X.

All hens were euthanized following VEGFR-2 targeted imaging and sonographic predictions were confirmed by gross examination of hens at necropsy. Gross morphology including the presence of ovarian follicles, atrophied ovaries and oviducts, presence of solid tumor mass in the ovary, extent of tumor metastasis, stages of OVCA and accompanying ascites, was recorded. Normal ovaries and ovaries with tumor together with other relevant tissues including oviducts were harvested and processed for paraffin, frozen, proteomic and molecular biological studies. Ovarian tumors and their types were confirmed by routine histological examination with hematoxylin-eosin staining (**Figure 2A-D**). Staging of ovarian tumors was performed as reported previously [6]. As predicted by sonographic examinations, late stage OVCA (n = 18 hens including 7 serous, 9 endometrioid, 2 mucinous) was accompanied with moderate to profuse ascites and metastasized to peritoneal and abdominal organs. In early stage OVCA (n = 8 including 3 serous, 4 endometrioid, 1mucinous) tumors were limited to the ovary with no or very little ascites. In addition, histological examinations confirmed the presence of microscopic ovarian carcinoma in 6 hens (3 serous and 3 endometrioid) that had no detectable ovarian mass during VEGFR-2 targeted gray scale scan as well as at gross. Thus the total number of hens with early stage OVCA was (8 + 6) = 14.

Immunohistochemical detection of ovarian tumor associated neo-angiogenic (TAN) markers:
Paraffin and frozen sections of normal ovaries or ovaries with tumor were immunostained for the detection of VEGFR-2+, SMA+, IL-16+ and CD8+ T cells using specific antibodies and the frequencies of the immunopositive vessels or cells were counted and analyzed as reported previously [10-12]. Differences in the frequency of immunopositive microvessels or cells between normal and hens with OVCA were considered significant when the $P < 0.05$.

Results: *Morphology of TAN vessels:* Neoangiogenic VEGFR-2 or SMA expressing microvessels were immature and appeared to be leaky with a discontinuous smooth muscle layer surrounding them.

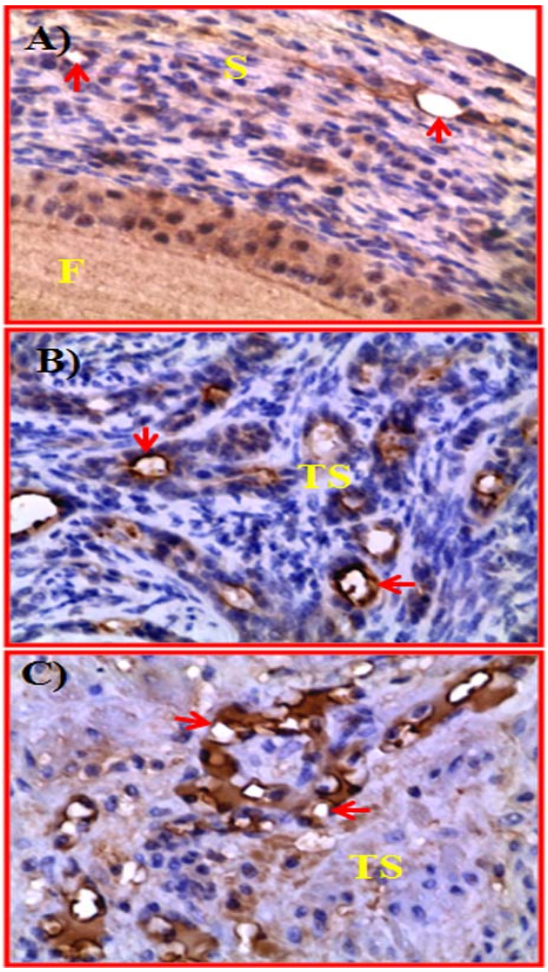

Figure 3. Immunohistochemical detection of vascular endothelial growth factor receptor-2 (VEGFR-2) expressing microvessels in a normal ovary or ovaries with tumors in hens. Sections were immunostained with anti-chicken VEGRF-2 antibodies. Microvessels expressing VEGFR-2 appear to be immature and leaky with incomplete or discontinous smooth muscle layers. Arrows show examples of VEGFR-2 expressing microvessels. A) Very few VEGFR-2 expressing microvessels are seen in the stroma of normal ovary. B-C) Compared with normal ovary (A), more VEGFR-2 expressing microvessels are seen in the stroma of the ovaries with tumor at early (B) and late (C) stages of OVCA. F = stromal follicle, S = stroma, TS = tumor stroma. 40X.

Expression of VEGFR-2 and SMA by TAN vessels: Microvessels expressing VEGFR-2 or SMA were localized at the spaces between tumor glands (tumor vicinity, **Figure 3B-C**). Occasionally ovarian tumor epithelia were also found positive for VEGFR-2 expression. The frequencies of VEGFR-2 expressing microvessels were significantly ($P<0.05$) greater in hens with early stage OVCA (mean ± SD= 12.8 ± 2.28 in 20,000μm^2 of tumor tissue) than in normal hens (3.12 ± 0.94 in 20,000μm^2 of ovarian stromal tissue) and increased further in hens with late stage of OVCA (18.33 ± 2.38 in 20,000μm^2 of tumor tissue) (**Figure 4**). Similar patterns of changes in the frequencies of SMA expressing microvessels were also observed. Differences in the frequencies of VEGFR-2 and SMA expressing microvessels were not observed among different histological sub-types of malignant ovarian tumors in hens. These results support the predictions of VEGFR-2 targeted imaging that VEGFR-2 expressing ovarian tumor associated microvessels can be detected *in vivo* and may be used as an imaging probe for the early detection of OVCA.

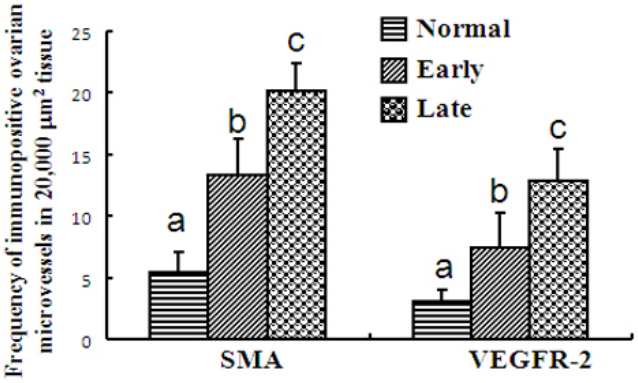

Figure 4. Changes in the frequencies of SMA and VEGFR-2 expressing microvessels in normal ovaries or ovaries with tumors in hens in association with ovarian tumor development and progression. Values are expressed as mean ± SD. Compared with normal ovaries (n = 15 hens), the frequencies of SMA and VEGFR-2 expressing microvessels were significantly greater in hens with early stage of ovarian cancer (OVCA, n = 14) ($P<0.01$) and increased further in hens with late stage OVCA (n = 18) ($P<0.01$). Patterns of changes in the frequency of SMA expressing cells are similar to that of VEGFR-2 expressing vessels. Bars with different letters within the same marker group are significantly different.

Detection of IL-16+ and CD8+ T cells: IL-16 is a chemoattractant and pro-angiogenic cytokine produced by a variety of cells including CD8 T cells. In normal ovaries, very few IL-16 expressing cells were seen in the ovarian stroma and the follicular theca. In contrast, many IL-16 expressing cells were localized in hens with OVCA (**Figure 5**). The population of IL-16 expressing cells was significantly ($P<0.05$) higher in hens with early stage OVCA (mean + SD= 16.30 ± 3.39in 20,000μm^2 of tumor tissue) than in normal hens (4.86 ± 0.95 in 20,000μm^2 of ovarian stromal tissue) and increased further in hens with late stage of OVCA (20.27 ± 4.58 in 20,000μm^2 of tumor tissue) (**Figure 6**).

CD8+ T cells were localized in the ovarian stroma and the theca layers of the stroma follicles while in ovaries with tumors they were localized in the tumor stroma as well as in close proximity to the tumor glands. A significantly higher frequency of CD8+ T cells was observed in hens with ovarian tumors than in hens with normal ovaries (**Figure 6**). The frequency of CD8+ T cells was 6 .00 ± 1.60 in 20,000μm^2 of ovarian stromal tissue (mean ± SD) in normal ovaries and increased significantly ($P<0.05$) in hens with early stage (mean ± SD= 24.92 + 6.69 in 20,000 μm^2 of tumor tissue) and late stages (27.07 + 4.52 in 20,000μm^2 of tumor tissue) of OVCA (**Figure 6**). The changes in the frequency of IL-16 positive cells are positively correlated with the changes in the frequency of CD8+ T cells as the tumor develops and progressed to late stages.

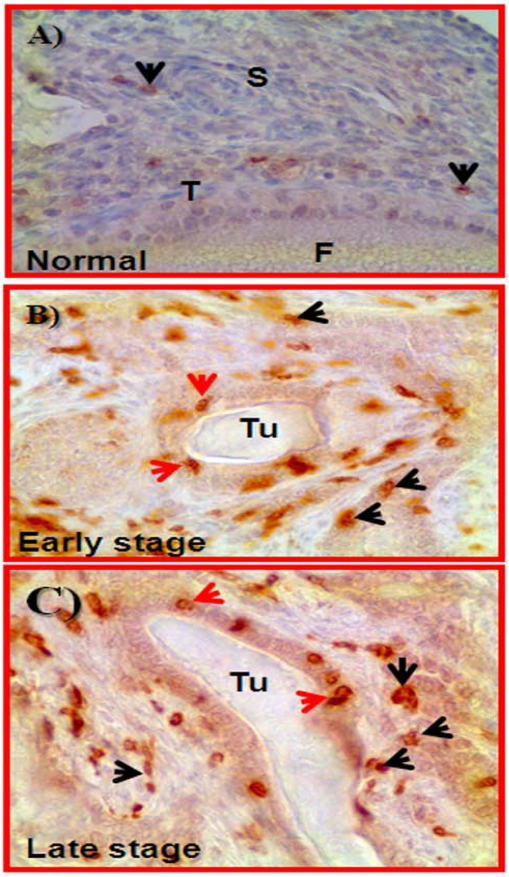

Figure 5. *Upper panel*: Immuno-histochemical localization of IL-16 expressing cells in the stroma of a normal ovary or ovaries with tumors in hens. Cells expressing IL-16 are round or irregularly shaped and seen in the normal ovarian or tumor stroma (arrows show the examples of IL-16+cells). A) Very few positive cells are seen in the stroma of normal ovary. B-C) IL-16 expression in early (B) and late (C) stages of OVCA in hens. A number of epithelial cells of the tumor also expressed IL-16 (red arrows). Compared with normal (A), more IL-16+ cells are seen in the stroma of the ovaries with tumor. S = ovarian stroma, Tu = tumor gland, 40X. T = theca layer of follicle (F).

Lower panel: Expression of IL-16 mRNA: Compared with weak expression by normal ovaries, strong expression of IL-16 mRNA was observed in homogenates from early and late stage OVCA.

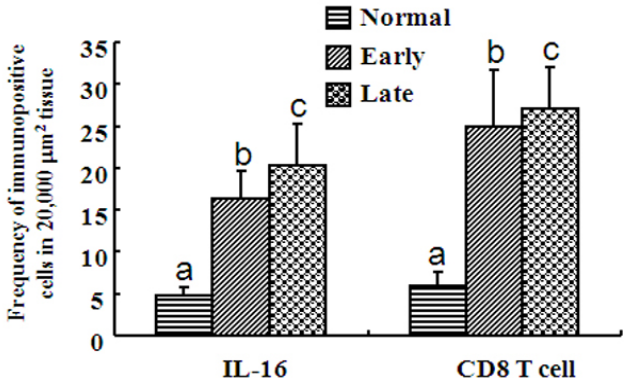

Figure 6. Changes in the frequencies of IL-16 expressing and CD8+ T cells in normal ovaries or ovaries with tumors in hens in association with ovarian tumor development and progression. Values are expressed as mean ± SD. Compared with normal ovaries (n = 15 hens), the frequencies of IL-16 expressing cells and CD8+ T cells were significantly greater in hens with early stage OVCA (n=14) ($P<0.01$) and increased further in hens with late stage OVCA (n=18) ($P<0.05$). Patterns of changes in the frequency of IL-16 expressing cells are positively correlated with that of CD8+ T cells. Bars with different letters within the same marker group are significantly different.

Thus the results of the immunohistochemical studies suggest that the frequencies of IL-16 expressing cells and their precursor (CD8+ T cells) increased in association with tumor development and progression.

Biochemical and molecular biological detection of malignant nuclear transformation and tumor associated neoangiogenesis:

Serum prevalence of anti-NMP antibodies: NMPs were extracted from normal ovaries and ovaries with tumors as reported previously [4]. 96-well plates were coated with NMPs and the immunoreactivities of serum samples from each hen against the coated normal or ovarian tumor NMPs were determined by immunoassay as reported earlier [13]. Each serum sample was assayed in duplicate and the plates were read at 405nm in an ELISA plate reader (Softmax Pro, version 1.2.0, software; Molecular Devices, Sunnyvale, CA). Serum from young healthy hens with fully functional ovaries was used as negative control (established in a previous study) for the presence of anti-NMP antibodies. Serum with optical density (OD) values higher than the control mean + 2SD (cut-off value) were considered positive for the presence of anti-NMP antibodies.

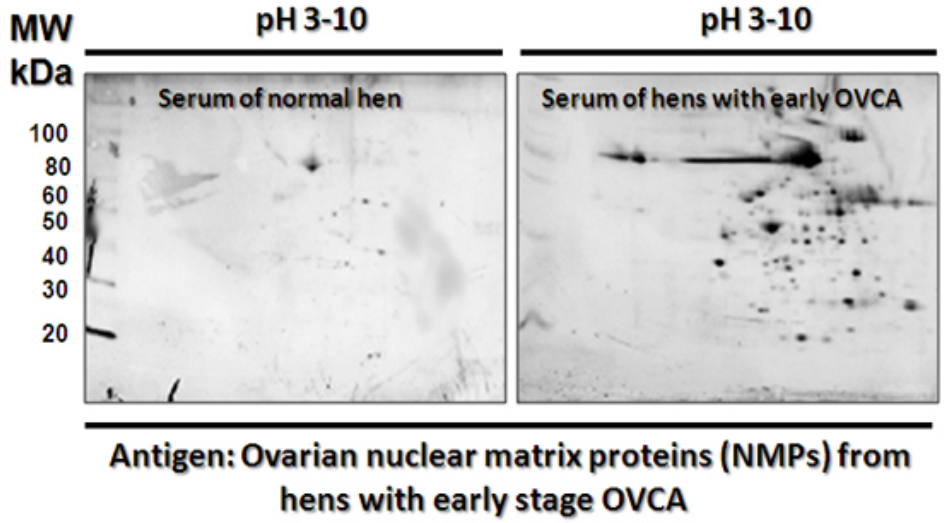

Figure 7. Immunoproteomic (2 dimensional Western blotting, 2D-WB) detection of anti-nuclear matrix protein (NMP) antibodies in the serum of hens with or without ovarian tumors. NMPs from hens with ovarian tumors were blotted in membranes and reacted with the serum of normal or OVCA hens. Compared with normal serum (left panel), OVCA serum reacted specifically against the ovarian tumor NMPs (most reactive antigens are seen approximately at 20-50kD) from OVCA hens.

All hens (n = 32) with OVCA were positive for anti-NMP antibodies while 5 normal hens (7.6%) hens were found positive for anti-NMP antibodies. Immunoreactivity observed in the immunoassay and OVCA specificity of the serum anti-NMP antibodies were tested by 2 dimensional Western blotting (2D-WB) as reported earlier[13]. Serum positive for anti-NMP antibodies from OVCA hens reacted specifically against NMPs from ovarian tumors (**Figure 7**) while very few immunoreactive spots were observed for hens with normal ovaries.

Serum levels of IL-16: Serum levels of IL-16 were determined by Chicken IL-16 Vetset™ ELISA Kit (Kingfisher Biotech, St. Paul, MN) pre-coated with anti-Chicken IL-16 antibodies and chicken IL-16 as standards as per the manufacturer's instructions reported earlier [12].The absorbance for each well was recorded by reading the plates at 405nm in a plate reader (Thermomax; Molecular Devices, Sunnyvale, CA). A standard curve was generated by plotting the optical density (OD) values of the standards against their concentrations. Serum IL-16 levels were determined with reference to the standard curve as per manufacturer's instruction using a software program (Softmax Pro, version 1.2.0, software; Molecular Devices, Sunnyvale, CA). All standards and serum samples were run in duplicate.

The mean concentration of serum IL-16 was 230.73 ± 47.01 pg/mL (mean ± SD) in normal hens. Compared with normal hens, the mean concentration of serum IL-16 was significantly higher ($P < 0.0002$) in hens with early (428.36 ± 136.53 pg/mL) and late stages (534.92 ± 204.62 pg/mL) of OVCA (**Figure 8**).

However, the differences in serum IL-16 levels were not significant between the early and late stages OVCA as well as among the different histological subtypes of OVCA.

IL-16 mRNA expression by normal ovaries or ovaries with tumor in hens: IL-16 mRNA expression was assessed by semi-quantitative RT-PCR as reported previously [12, 14] using chicken-specific IL-16 primers designed by Oligoperfect Designer software (Invitrogen, Carlsbad, CA) with the IL-16 sequence from the NCBI (GeneBank: NM_204352.3). The forward primer was 5-TCTCTGCTTTCCCCTGAA-GA and the reverse primer was 5-GTCCATTGGGAAACACCT-TG located between exons 4 and 6. β-actin was used as the endogenous control with a forward primer of TGCGTGACATCAAGGAGAAG and a reverse primer of ATGCCAGGGTACATTGTGGT. The expected base pair size for the IL-16 amplicon was 199 bp and for β-actin was 300 bp. PCR amplicons were visualized in a 3% agarose gel (Pierce/Thermo Fisher, Rockford, IL USA) in TAE buffer and stained with ethidium bromide. The image was captured using a ChemiDoc XRS system (Bio-Rad, Hercules, CA).

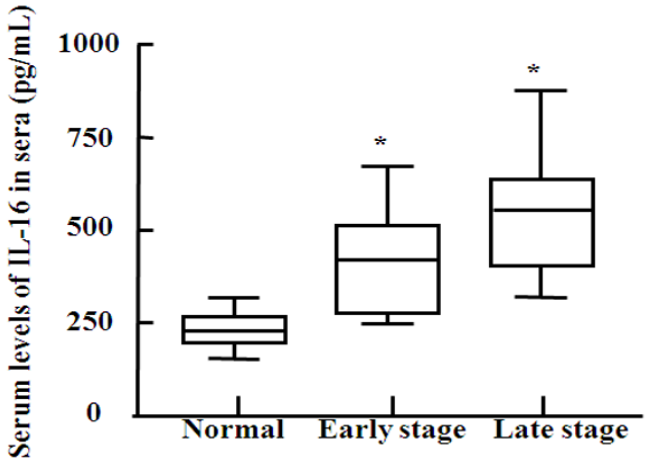

Figure 8. Serum levels of IL-16 (pg/mL) in hens with or without ovarian cancer (OVCA) displayed as box and whiskers. The median, range (whiskers), and 25th to 75th percentiles (box) are shown. Serum samples from normal hens were used as experimental controls. Compared with normal hens (n = 66), serum IL-16 levels was significantly greater (P<0.0002) in hens with early (n = 14) and late (n = 18) stages of OVCA. * denotes significant differences in the serum IL-16 levels between normal hens and hens with OVCA.

IL-16 mRNA expression was weak for ovarian homogenates from normal hens. In contrast, hens with ovarian tumors showed a strong amplification signal for IL-16 (**Figure 5**) and differences were not observed in IL-16 mRNA expression among different histological subtypes of OVCA. Thus, IL-16 mRNA expression confirmed the observed variations in serum IL-16 levels and ovarian expression of IL-16 among normal and OVCA hens.

Ovarian TAN Index (TI): The patterns of tumor associated changes in the frequencies of VEGFR-2 expressing microvessels were found to be similar in OVCA hens irrespective of tumor sub-types. A tumor associated neoangiogenic index indicative of OVCA with reference to histopathology was calculated as: TI = Number of VEGFR-2 positive cells in [tumor ovaries/normal ovaries]. Compared with normal hens, the mean TI for early stage and late stage OVCA was significantly higher (4.26 vs 1.00, P <0.01) and (6.26 vs 1.00, P < 0.01), respectively. Considering the TI values for normal as 1 (number of VEGFR-2 expressing vessels in normal hens/ number of VEGFR-2 expressing vessels in normal), these TI values are higher than 2X of TI of normal hens. In addition, the population of VEGFR-2 expressing microvessels in hens with early stage OVCA (mean + SD = 12.8 + 2.28 in 20,000 μm^2 area) is greater than the 2 X mean of normal hens + 2SD (= 2 X 3.12 + 2X0.94 = 8.12). Thus, it is assumed that the TI for early stage OVCA shown above (4.26) will effectively identify ovarian TAN in early stage OVCA. Moreover, TI was inversely associated with Doppler indices from OVCA hens (the higher the TI, the lower the RI and PI) indicating that development of ovarian TAN is associated with an increase in blood flow to the tumor tissue. Overall, the early stage OVCA diagnostic indices established with reference to histopathology and ovarian expression of TAN markers are:

a. Pixel intensities diagnostic of early stage OVCA from VEGFR-2 targeted molecular ultrasound imaging: 10,500 pixels or higher

b. Doppler indices diagnostic of early stage OVCA from VEGFR-2 targeted ultrasound molecular imaging: RI = 0.44 or lower
c. Serum IL-16 level: Diagnostic levels of serum IL-16 for early stage OVCA = 450 pg/mL or higher based on corresponding histopathological diagnosis of ovarian tumors.

KEY RESEARCH ACCOMPLISHMENTS:

- Enhancement of OVCA detectability of traditional ultrasound scanning by VEGFR-2 targeted molecular imaging agents.
- Confirmed the binding of targeted imaging agents to the tissue marker of ovarian tumor associated neoangiogenesis (microvessels expressing VEGFR-2) in a preclinical model of spontaneous ovarian cancer.
- Ultrasound prediction of tumor related overexpression of ovarian VEGFR-2 confirmed by immunohistochemical detection.
- OVCA diagnostic level of serum IL-16, a novel marker of tumor associated neoangiogenesis at early stage was determined by an immunoassay.
- Using immunoproteomics and gene expression, this study has shown that ovarian tumor epithelium may be a source of serum IL-16 in this animal model.
- This study also showed that serum anti-NMP antibodies are associated with the early ovarian tumor development.

REPORTABLE OUTCOMES:

Presentation: Abstract published and presented: (*link provided*)

1. **Barua A**, Qureshi T, Bitterman P, Bahr JM, Basu S, Edassery SL, Abramowicz JS, (2012) Molecular targeted imaging of vascular endothelial growth factor receptor (VEGFR)-2 and anti-NMP autoantibodies detect ovarian tumor at early stage. American Association for Cancer Research annual meeting, 2012; March 3^{1st} to April ^{4th}, 2012, McCormick Place, Chicago, IL. Abstract ID# 2455; http://cancerres.aacrjournals.org/cgi/content/meeting_abstract/72/8_MeetingAbstracts/2455

Manuscript: One manuscript is under preparation.

CONCLUSION:

The results so far obtained with the accomplishment of Aim 1 suggest that VEGFR-2 targeted ultrasound molecular imaging probes enhanced the detection of ovarian malignant tumors as well as ovarian tumor associated neoangiogenesis in laying hen model of spontaneous ovarian cancer (OVCA). This study also showed that anti-NMP antibodies are prevalent in association with ovarian tumor development. Elevated serum levels of IL-16 was associated with the increase in OVCA related targeted imaging indices. VEGFR-2 targeted ultrasound molecular indices and IL-16 serum levels detective of OVCA established in Aim 1 are being tested in Aim 2 for the detection of OVCA at early stage.

REFERENCES

1. Jemal A, Siegel R, Xu J, and Ward E. Cancer statistics, 2010. *CA Cancer J Clin* 2010; 60: 277-300.
2. Ries LA. Ovarian cancer. Survival and treatment differences by age. *Cancer* 1993; 71: 524-9.
3. Moore RG and Bast RC, Jr. How do you distinguish a malignant pelvic mass from a benign pelvic mass? Imaging, biomarkers, or none of the above. *J Clin Oncol* 2007; 25: 4159-61.
4. Yu E, Lee H, Oh W, Yu B, Moon H, and Lee I. Morphological and biochemical analysis of anti-nuclear matrix protein antibodies in human sera. *J Korean Med Sci* 1999; 14: 27-33.
5. Vanderhyden BC, Shaw TJ, and Ethier JF. Animal models of ovarian cancer. *Reprod Biol Endocrinol* 2003; 1: 67.
6. Barua A, Bitterman P, Abramowicz JS, Dirks AL, Bahr JM, Hales DB, Bradaric MJ, Edassery SL, Rotmensch J, and Luborsky JL. Histopathology of ovarian tumors in laying hens: a preclinical model of human ovarian cancer. *Int J Gynecol Cancer* 2009; 19: 531-9.
7. Barua A, Abramowicz JS, Bahr JM, Bitterman P, Dirks A, Holub KA, Sheiner E, Bradaric MJ, Edassery SL, and Luborsky JL. Detection of ovarian tumors in chicken by sonography: a step toward early diagnosis in humans? *J Ultrasound Med* 2007; 26: 909-19.
8. Barua A, Bitterman P, Bahr JM, Basu S, Sheiner E, Bradaric MJ, Hales DB, Luborsky JL, and Abramowicz JS. Contrast-enhanced sonography depicts spontaneous ovarian cancer at early stages in a preclinical animal model. *J Ultrasound Med* 2010; 30: 333-45.
9. Anderson CR, Hu X, Zhang H, Tlaxca J, Decleves AE, Houghtaling R, Sharma K, Lawrence M, Ferrara KW, and Rychak JJ. Ultrasound molecular imaging of tumor angiogenesis with an integrin targeted microbubble contrast agent. *Invest Radiol*; 46: 215-24.
10. Barua A, Bitterman P, Bahr JM, Basu S, Sheiner E, Bradaric MJ, Hales DB, Luborsky JL, and Abramowicz JS. Contrast-enhanced sonography depicts spontaneous ovarian cancer at early stages in a preclinical animal model. *J Ultrasound Med* 2011; 30: 333-45.
11. Barua A and Yoshimura Y. Effects of aging and sex steroids on the localization of T cell subsets in the ovary of chicken, Gallus domesticus. *Gen Comp Endocrinol* 1999; 114: 28-35.
12. Yellapa A, Bahr JM, Bitterman P, Abramowicz JS, Edassery SL, Penumatsa K, Basu S, Rotmensch J, and Barua A. Association of interleukin 16 with the development of ovarian tumor and tumor-associated neoangiogenesis in laying hen model of spontaneous ovarian cancer. *Int J Gynecol Cancer* 2012; 22: 199-207.
13. Barua A, Edassery SL, Bitterman P, Abramowicz JS, Dirks AL, Bahr JM, Hales DB, Bradaric MJ, and Luborsky JL. Prevalence of antitumor antibodies in laying hen model of human ovarian cancer. *Int J Gynecol Cancer* 2009; 19: 500-7.
14. Hong YH, Lillehoj HS, Lee SH, Dalloul RA, and Lillehoj EP. Analysis of chicken cytokine and chemokine gene expression following Eimeria acervulina and Eimeria tenella infections. *Vet Immunol Immunopathol* 2006; 114: 209-23.